International Journal of Hyperthermia

ISSN: 0265-6736 (Print) 1464-5157 (Online) Journal homepage: informahealthcare.com/journals/ihyt20

^{18}F-FET PET for planning of thermotherapy using magnetic nanoparticles in recurrent glioblastoma

Hot Topic

Michail Plotkin, Uwe Gneveckow, Klaus Meier-Hauff, Holger Amthauer, Annelie Feußner, Timm Denecke, Matthias Gutberlet, Andreas Jordan, Roland Felix & Peter Wust

To cite this article: Michail Plotkin, Uwe Gneveckow, Klaus Meier-Hauff, Holger Amthauer, Annelie Feußner, Timm Denecke, Matthias Gutberlet, Andreas Jordan, Roland Felix & Peter Wust (2006) ^{18}F-FET PET for planning of thermotherapy using magnetic nanoparticles in recurrent glioblastoma, International Journal of Hyperthermia, 22:4, 319-325, DOI: 10.1080/02656730600734128

To link to this article: https://doi.org/10.1080/02656730600734128

Published online: 09 Jul 2009.

Submit your article to this journal

Article views: 888

View related articles

Citing articles: 6 View citing articles

Full Terms & Conditions of access and use can be found at
https://informahealthcare.com/action/journalInformation?journalCode=ihyt20

Int. J. Hyperthermia, June 2006; 22(4): 319–325

Taylor & Francis
Taylor & Francis Group

HOT TOPIC

^{18}F-FET PET for planning of thermotherapy using magnetic nanoparticles in recurrent glioblastoma

MICHAIL PLOTKIN[1], UWE GNEVECKOW[2], KLAUS MEIER-HAUFF[3], HOLGER AMTHAUER[1], ANNELIE FEUßNER[1], TIMM DENECKE[1], MATTHIAS GUTBERLET[1], ANDREAS JORDAN[2], ROLAND FELIX[1], & PETER WUST[1]

[1]*Department of Radiology, Nuclear Medicine and Radiooncology, Campus Virchow-Klinikum, Charité – Universitätsmedizin Berlin, Germany,* [2]*MagForce Nanotechnologies AG, Berlin, Germany, and* [3]*Department of Neurosurgery, Bundeswehrkrankenhaus Berlin, Germany*

(Received 19 February 2006; revised 29 March 2006; accepted 3 April 2006)

Abstract

Purpose: Thermotherapy using magnetic nanoparticles (nano cancer therapy) is a new concept of local tumour therapy, which is based on controlled heating of intra-tumoural injected magnetic nanoparticles. The aim of this study was to evaluate the usefulness of PET with a recently introduced amino acid tracer O-(2-[^{18}F]fluoroethyl)-L-tyrosine (FET) for targeting the nanoparticles implantation.

Materials and methods: Eleven patients with glioblastoma recurrences underwent MR and FET-PET imaging for planning of the nano cancer therapy. Thereafter, the gross tumour volumes (GTV) were defined, taking into consideration the results of both imaging tools.

Results: The MRI-based mean GTV was 24.3 cm^3 (range 2.5–59.7) and the PET-based mean GTV 31.9 cm^3 (range 5.2–77.9). On the average the MRI identified an additional 8.9 ± 4.7 cm^3 and the FET-PET scan—an additional 16.5 ± 15.2 cm^3 outside of the common GTV (15.4 ± 11.0 cm^3). The mean final GTV accounted to 33.8 cm^3 (range, 5.2–77.9). The additional information of FET-PET led to an increase in GTV by 22–286% in eight patients and to a decrease of 23% and 26%, respectively, in two patients. In one patient, the final GTV was defined on the basis of MRI data only.

Conclusions: FET-PET adds important information on the actual tumour volume in recurrent glioblastomas and is highly valuable for defining the target volume for the nano cancer therapy.

Keywords: *^{18}F-FET, positron emission topography, recurrent glioblastoma, nano cancer therapy*

Correspondence: M. Plotkin, MD, Klinik für Strahlenheilkunde, Universitätsklinik Charité Campus Virchow-Klinikum Augustenburger Platz 1, 13353 Berlin, Germany. Tel: +49 030 450-557 679. Fax: +49 030 450-557 909. E-mail: michail.plotkin@charite.de

ISSN 0265–6736 print/ISSN 1464–5157 online © 2006 Taylor & Francis
DOI: 10.1080/02656730600734128

Introduction

Thermotherapy using magnetic nanoparticles (designated nano cancer therapy) is a new approach of localized thermotherapy, in which nanosized iron-oxide particles are directly injected into a tumour and subsequently heated in an alternating magnetic field. This method was developed by Jordan and co-workers [1–3], who carried out comprehensive pre-clinical investigations, which proved the feasibility and effectiveness of this innovative approach for the treatment of diverse malignancies, including prostate cancer, breast cancer and glioma [1, 4–7]. Clinical studies were initiated [8] and their first results support the potential value of the nano cancer therapy for successful treatment of tumours in deep body regions.

An important pre-requisite for the successful nano cancer therapy is the coverage of the whole tumour volume with magnetic nanoparticles, which is required for sufficient heat deposition. In case of recurrent glioblastomas, the viable tumour tissue should be exactly delineated and differentiated from therapy-induced tissue alterations such as peritumoural oedema, post-operative scar and radiation necrosis. MRI is of limited ability at this task [9, 10]. Nuclear medicine imaging (SPECT, PET) with amino acids tracers provides essential information on tumour metabolism and was shown to be highly valuable for diagnosis of recurrent glioma [11–16]. Its usefulness for planning of radiation therapy of primary and recurrent gliomas was already proven by several investigations [17–21]. PET using the recently introduced amino acid tracer O-(2-[^{18}F]fluoroethyl)-L-tyrosine (FET) allows a more precise estimation of tumour borders than MRI [22]. Although the FET is not incorporated into proteins and its accumulation only reflects amino acid transport, the uptake of FET has been shown to be closely correlated with that of the well-studied PET tracer of protein synthesis ^{11}C-methionine [23]. The ^{11}C-methionine is of limited availability due to the short physical half-life of the ^{11}C label and can be used only in few PET centres, equipped with a cyclotron. Therefore, the FET, which is labelled with ^{18}F (half-life, 110 min) represents a reasonable alternative to ^{11}C-methionine for the clinical applications. The advantage of the FET-PET over the SPECT using ^{123}I-iodo-methyl-thyrosine is the improved discrimination of anatomic structures and the better tumour-to-brain contrast [24].

The aim of the present study was to investigate the impact of FET-PET on planning of nano cancer therapy of recurrent glioblastomas.

Materials and methods

Patients

Included were 11 consecutive patients (four females, seven males; median age 44 years, range 25–75 years) with recurrent glioblastomas, who were candidates for nano cancer therapy. The inclusion criteria were a Karnofsky index ≥ 60, expansion of the tumour to a maximum of 6 cm and supratentorial and unifocal localization. Patient characteristics and pre-treatment data are given in Table I. In all patients, failure of the initial treatment was estimated based on serial MRI scans (interval to PET examination <3 days). A written informed consent was obtained from all patients for the PET examinations. The study was approved by the local ethical committee.

Methods

PET studies were performed using an ECAT-EXACT 47 scanner. The patients took a protein-low diet for 8 h prior to PET investigation. Transmission scans using a ^{68}Ge/^{68}Ga

Table I. Demographic data and history of 11 patients with recurrent glioblastoma.

Pat. No.	Age (years)	Sex	Location	Pre-treatment
1	34	F	R FL	Surg, Rad, Chemo
2	57	M	L TL	Surg, Rad
3	25	M	L Thalamus	Surg, Rad, Chemo
4	55	M	L FL	Surg
5	69	M	L TL	Surg, Rad, Chemo
6	44	F	L OL	Surg, Chemo
7	41	M	L TL	Surg, Rad
8	38	F	L FL	Surg, Rad, Chemo
9	40	M	R FL	Surg, Rad, Chemo
10	75	F	L TL	Surg, Rad, Chemo
11	58	M	L TL	Surg, Rad, Chemo

M = male; F = female; L = left side; R = right side; FL = frontal lobe; TL = temporal lobe; OL = occipital lobe; Surg = Surgery; Rad = Radiation therapy; Chemo = Chemotherapy.

rod source were collected immediately after intravenous administration of 250 MBq ^{18}F-FET (acquisition time 10 min). Thereafter, emission scans were acquired for 30 min. PET slices were reconstructed by filtered back projection using a Hanning filter (cut-off 0.4).

After coregistering of PET and MRI data, the gross tumour volumes (GTV) were delineated separately, based on MRI and PET data. The GTV were delineated manually in the MR images as areas with Gd-enhancement and in the fused MRI/PET images as areas showing activity concentration above 75% of the maximal value inside the tumour. Thereafter, the final GTV were defined in the fused MRI/PET images, taking into consideration the results of both imaging tools as well as individual anatomical and clinical particulars. The resulting data were transferred to the neurosurgical navigation system (Stealth Station, Medtronic, MN) and used for stereotactic guidance of the nanoparticles instillation. Thereby three-to-nine cylindrical nanoparticle depots were placed within the GTV following a pre-instillation plan created by *Nanoplan*® (MagForce Nanotechnologies AG, Berlin, Germany), a 3-dimensional AMIRA-based software for nano cancer therapy. The common GTV of FET-PET and MRI and the final GTV were measured in fused MRI/PET images. Intra-individual differences in GTV between both modalities were analysed using a paired *t*-test, considering a p value < 0.05 as statistically significant (SPSS v. 10 (Chicago, IL)).

Results

The individual volumes and differences in the GTV between FET-PET and MRI are given in Table II. The mean GTV, as estimated in MRI, was 24.3 cm^3 (range 2.5–59.7 cm^3), whereas the mean GTV in the PET-based planning was 31.9 cm^3 (range 5.2–77.9 cm^3). The difference was not statistically significant ($p = 0.072$). Taking the common GTV into account, FET-PET revealed an average of 16.5 cm^3 as additional GTV and did not cover an average of 8.9 cm^3 of the MRI defined GTV.

The mean final GTV which was used for nano cancer therapy planning was 33.8 cm^3 (range 5.2–59.7 cm^3). The implementation of FET-PET data led to the increase in the mean final GTV by 9.4 cm^3, as compared to volumes determined with MRI only. Looking at the individual therapy planning, the final GTV was increased by 22–286% in eight patients

Table II. Results of volumetric measurements using Gd-enhanced MRI and FET-PET in 11 patients with recurrent glioblastomas.

	GTV MRI (cm^3)	GTV FET (cm^3)	Common GTV (cm^3)	GTV MRI less common GTV (cm^3)	GTV FET less common GTV (cm^3)	Final GTV (cm^3)	Change in GTV by FET-PET (cm^3/%)
1	59.7	76.8	39.7	20.0	37.1	59.7	0*
2	11.3	43.6	6.2	5.1	37.4	43.6	+32.3/+286
3	2.5	5.2	1.9	0.6	3.3	5.2	+2.7/+108
4	15.1	18.3	9.3	5.8	9.0	24.1	+9.0/+60
5	39.9	40.2	31.3	8.6	8.9	48.5	+8.7/+22
6	44.0	26.2	19.6	14.4	6.6	26.2	−7.8/−23
7	13.6	14.8	6.6	7.0	8.2	22.0	+8.4/+62
8	31.7	23.3	17.5	14.2	5.8	23.3	−8.4/−26
9	19.9	18.4	6.4	13.5	12.0	30.7#	+10.8/−54#
10	5.3	6.6	1.2	4.1	5.4	10.7	+5.4/+102
11	34.8	77.9	30.1	4.7	47.8	77.9#	+43.1/+128#
Mean	24.3	31.9	15.4	8.9	16.5	33.8	+9.4
SD	13.3	21.7	11.0	4.7	15.2	20.9	16.8(±79%)

GTV = gross tumour volume; SD = standard deviation.
*The additional volume, defined using FET-PET, was not accessible for nano cancer therapy and thus did not contribute to the PV; # no therapy was performed; ± mean percentage change (absolute value).

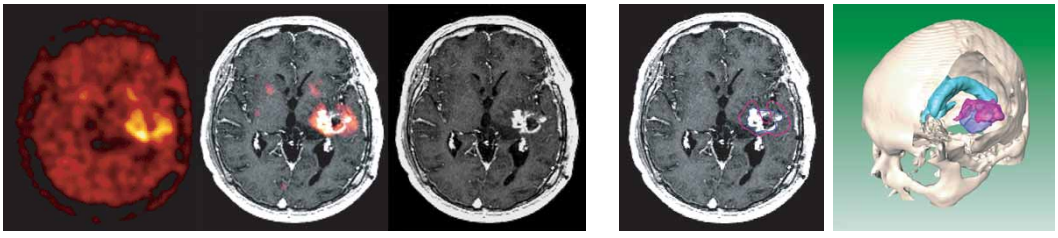

Figure 1. A 41-year-old male patient (No. 7) suffering from recurrent glioblastoma in the left temporal lobe. The FET-PET scan (A) shows a larger tumour extension than the corresponding Gd-enhanced MR scan (C); see also the fused image (B). The discrepancies between tumour borders, defined on the PET and MR scans, are shown in the transversal MR image (D) and in the 3D surface-based reconstruction (E). The blue-coloured line/surface marks the MRI-based tumour borders and the rose-coloured line/surface marks the PET-based tumour borders. The green-coloured surface in the image E marks the ventricular system.

(a representative case is shown in Figure 1) and decreased in two patients by 23% and 26%, respectively. The observed relation between the MRI- and PET-based volumes was in the individual cases complex: in five out of eight patients, whose overall final GTV was increased by FET PET, some Gd-enhancing, but FET negative areas were found as well (Pat. No. 2, 4, 5, 7, 10, Table II). In two of the 11 studied patients, FET-PET showed no viable tumour in the areas which showed growth in the previous serial MRI investigations. The mean percentage of therapy relevant GTV alteration was 79%. In one patient (No. 1), FET-PET demonstrated a bihemispheric spread of the tumour with infiltration of the sagittal sinus, which was not detected by MRI. The additional tumour volume shown by FET-PET was not accessible for implantation of nanoparticles and, therefore, did not contribute to the

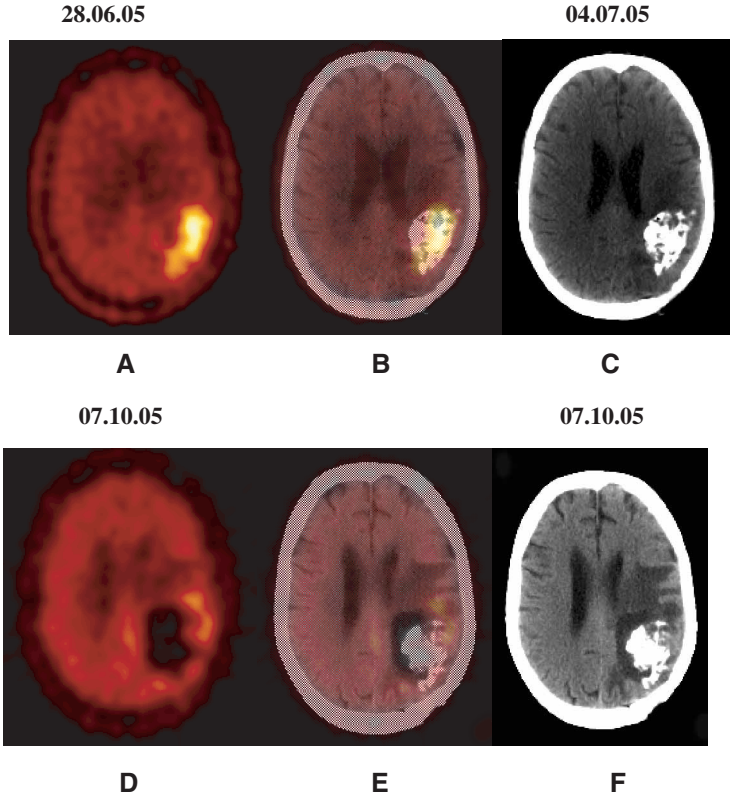

Figure 2. A 44-year-old female patient (No. 6) with recurrent glioblastoma in the left occipital lobe, showing an increased amino acid accumulation (A). CT examination (C), performed 1 day after PET-guided injection of nanoparticles and the fused PET/CT scan (B) allow assessment of their distribution. The control examinations 13 weeks after nano cancer therapy (D–F) show a significant reduction in the amino acid accumulation (PET) and building of necrotic/oedematous zones around the nanoparticles deposits (CT).

final GTV. In two of the 11 patients, the nano cancer therapy was not performed owing to unexpected extensive tumour spread demonstrated by FET-PET (Pat. No. 11) and because of incompliance (Pat. No. 9).

Discussion

The particularity of planning the nano cancer therapy of recurrent glioblastomas owes to the definition of the target volume for instillation of the nanoparticles. The visible tumour mass (GTV) was the basis of planning the nano particle depot position. One took care during the planning process to ensure a safety margin between a selected isotherm and the GTV. In this study, FET-PET influenced the therapy planning, leading to a change of the final GTV in 10/11 patients (the mean change accounted for 74%). In one patient (No. 11), the results of PET investigation lead to modification of the therapeutic strategy. The lack of statistical significance of differences between the MRI- and PET-based GTV in this study can be explained by the relatively small number of patients. Another possible reason might be

related to the presence of bi-directional changes in GTV when comparing MRI to FET-PET, both at the inter-individual and intra-individual level. Indeed, on the average, the MRI identified an additional $8.9 \pm 4.7\,cm^3$ and the FET-PET scan—an additional $16.5 \pm 15.2\,cm^3$ outside of the common GTV ($15.4 \pm 11.0\,cm^3$). The fact that the inclusion of the FET-PET data in the therapy planning led to an increase rather then a decrease in the final GTV (mean increase was $9\,cm^3$) is in accordance with the results of Grosu et al. [17], who found the mean relative increase in PTV by $5\,cm^3$ using ^{123}I-IMT SPECT. The pathophysiological explanation for this phenomenon is most likely an increased amino acid uptake of tumour tissue without a brain-barrier disruption. This consideration is backed by the results of the histopathology-based studies by Pauleit et al. [22] and Kracht et al. [21], which showed amino acid accumulation being a more reliable indicator for the presence of tumour tissue than a brain-barrier damage, detected by the contrast enhancement in MRI. The less commonly observed appearance of contrast enhancing regions in areas without amino acid uptake can be explained by a non-specific breakdown of the blood–brain barrier following surgery and radiation therapy [11, 13, 14, 21].

Apart from the superior definition of the tumour volume, the rationale for the use of the ^{18}F-FET-PET in planning of the nano cancer therapy is the suitability for post-treatment evaluation (see example in Figure 2), since MRI cannot be used post-treatment because of susceptibility artifacts, caused by the magnetic nanoparticles. The usefulness of FET-PET for evaluation of the response to the nano cancer therapy is currently under investigation in the clinic.

Conclusion

FET-PET, as an adjunctive to MRI, reveals relevant information for therapy planning in patients with recurrent glioblastoma and thus proves to be valuable as a planning tool for novel therapy approaches such as nanoparticle mediated hyperthermia.

References

1. Jordan A, Scholz R, Wust P, Fahling H, Krause J, Wlodarczyk W, Sander B, Vogl T, Felix R. Effects of magnetic fluid hyperthermia (MFH) on C3H mammary carcinoma *in vivo*. Int J Hyperthermia 1997;13:587–605.
2. Jordan A, Wust P, Scholz R, Tesche B, Fahling H, Mitrovics T, Vogl T, Cervos-Navarro J, Felix R. Cellular uptake of magnetic fluid particles and their effects on human adenocarcinoma cells exposed to AC magnetic fields *in vitro*. Int J Hyperthermia 1996;12:705–722.
3. Gneveckow U, Jordan A, Scholz R, Bruess V, Waldoefner N, Ricke J, Feussner A, Hildebrandt B, Rau B, Wust P. Description and characterization of the novel hyperthermia- and thermoablation-system MFH 300F for clinical magnetic fluid hyperthermia. Med Phys 2004;31:1444–1451.
4. Jordan A, Scholz R, Maier-Hauff K, van Landeghem FK, Waldoefner N, Teichgraeber U, Pinkernelle J, Bruhn H, Neumann F, Thiesen B, von Deimling A, Felix R. The effect of thermotherapy using magnetic nanoparticles on rat malignant glioma. J Neurooncol 2005;29:1–8.
5. Johannsen M, Jordan A, Scholz R, Koch M, Lein M, Deger S, Roigas J, Jung K, Loening S. Evaluation of magnetic fluid hyperthermia in a standard rat model of prostate cancer. J Endourol 2004;18:495–500.
6. Johannsen M, Thiesen B, Jordan A, Taymoorian K, Gneveckow U, Waldoefner N, Scholz R, Koch M, Lein M, Jung K, Loening SA. Magnetic fluid hyperthermia (MFH) reduces prostate cancer growth in the orthotopic Dunning R3327 rat model. Prostate 2005;64:283–292.
7. Johannsen M, Thiesen B, Gneveckow U, Taymoorian K, Waldoefner N, Scholz R, Deger S, Jung K, Loening SA, Jordan A. Thermotherapy using magnetic nanoparticles combined with external radiation in an orthotopic rat model of prostate cancer. Prostate 2006;66:97–104.

8. Johannsen M, Gneveckow U, Eckelt L, Feussner A, Waldoefner N, Scholz R, Deger S, Wust P, Loening SA, Jordan A. Clinical hyperthermia of prostate cancer using magnetic nanoparticles: Presentation of a new interstitial technique. Int J Hyperthermia 2005;21:637–647.
9. Leeds NE, Jackson EF. Current imaging techniques for the evaluation of brain neoplasms. Curr Opin Oncol 1994;6:254–261.
10. Kelly PJ, Daumas-Duport C, Scheithauer BW, Kall BA, Kispert DB. Stereotactic histologic correlations of computed tomography- and magnetic resonance imaging-defined abnormalities in patients with glial neoplasms. Mayo Clin Proc 1987;62:450–459.
11. Samnick S, Bader JB, Hellwig D, Moringlane JR, Alexander C, Romeike BF, Feiden W, Kirsch CM. Clinical value of iodine-alpha-methyl-L-thyrosine single-photon emission tomography in the differential diagnosis of recurrent brain tumor in patients pretreated for glioma at follow-up. J Clin Oncol 2002;20:396–404.
12. Kuwert T, Woesler B, Morgenroth C, Lerch H, Schafers M, Palkovic S, Matheja P, Brandau W, Wassmann H, Schober O. Diagnosis of recurrent glioma with SPECT and iodine-123-alpha-methyl tyrosine. J Nucl Med 1998;39:23–27.
13. Plotkin M, Eisenacher J, Bruhn H, Wurm R, Michel R, Stockhammer F, Feußner A, Dudeck O, Wust P, Felix R, Amthauer H. ^{123}I-IMT SPECT and ^{1}H MR-spectroscopy at 3.0 Tesla in the differential diagnosis of recurrent or residual gliomas: A comparative study. J Neuro Oncol 2004;70:49–58.
14. Plotkin M, Amthauer H, Eisenacher J, Wurm R, Michel R, Wust R, Stockhammer F, Gutberlet M, Röttgen R, Ruf J, Felix R. Value of ^{123}I-IMT SPECT for diagnosis of recurrent non-astrocytic intracranial tumours. Neuroradiology 2005;47:18–26.
15. Amthauer H, Wurm R, Kuczer D, Ruf J, Michel R, Eisenacher J, Stockhammer F, Denecke T, Felix R, Plotkin M. Relevance of image fusion with MRI for the interpretation of ^{123}I-IMT scans in patients with suspected recurrent or residual brain tumors. Clin Nucl Med 2006;31:189–192.
16. Popperl G, Gotz G, Rachinger W, Gildehaus FJ, Tonn JC, Tatsch K. Value of O-(2-[^{18}F]fuoroethyl)-L-tyrosine PET for the diagnosis of recurrent glioma. Eur J Nucl Med Mol Imag 2004;11:1464–1470.
17. Grosu AL, Feldmann H, Dick S, Dzewas B, Nieder C, Gumprecht H, Frank A, Schwaiger M, Molls M, Weber WA. Implications of IMT-SPECT for postoperative radiotherapy planning in patients with gliomas. Int J Radiat Oncol Biol Phys 2002;54:842–854.
18. Grosu AL, Weber WA, Riedel E, Jeremic B, Nieder C, Franz M, Gumprecht H, Jaeger R, Schwaiger M, Molls M. L-(methyl-^{11}C) methionine positron emission tomography for target delineation in resected high-grade gliomas before radiotherapy. Int J Radiat Oncol Biol Phys 2005;63:64–74.
19. Nuutinen J, Sonninen P, Lehikoinen P, Sutinen E, Valavaara R, Eronen E, Norrgard S, Kulmala J, Teras M, Minn H. Radiotherapy treatment planning and long-term follow-up with [(11)C] methionine PET in patients with low-grade astrocytoma. Int J Radiat Oncol Biol Phys 2000;48:43–52.
20. Grosu AL, Weber WA, Franz M, Stark S, Piert M, Thamm R, Gumprecht H, Schwaiger M, Molls M, Nieder C. Reirradiation of recurrent high-grade gliomas using amino acid PET (SPECT)/CT/MRI image fusion to determine gross tumor volume for stereotactic fractionated radiotherapy. Int J Radiat Oncol Biol Phys 2005;63:511–519.
21. Kracht LW, Miletic H, Busch S, Jacobs AH, Voges J, Hoevels M, Klein JC, Herholz K, Heiss WD. Delineation of brain tumor extent with [^{11}C]L-methionine positron emission tomography: Local comparison with stereotactic histopathology. Clin Cancer Res 2004;10:7163–7170.
22. Pauleit D, Floeth F, Hamacher K, Riemenschneider MJ, Reifenberger G, Muller HW, Zilles K, Coenen HH, Langen KJ. O-(2-[^{18}F]fluoroethyl)-L-tyrosine PET combined with MRI improves the diagnostic assessment of cerebral gliomas. Brain 2005;128:678–687.
23. Weber W, Wester HJ, Grosu AL, Herz M, Dzewas B, Feldmann HJ, Molls M, Stocklin G, Schwaiger M. O-(2-[^{18}F] fluoroethyl)-L-tyrosine and L-[methyl-^{11}C] methionine uptake in brain tumours: Initial results of a comparative study. Eur J Nucl Med 2000;27:542–549.
24. Pauleit D, Floeth F, Tellmann L, Hamacher H, Hautzel H, Müller HW, Coenen HH, Langen KJ. Comparison of O-(2-^{18}F-fluoroethyl)-L-tyrosinePET and 3-123I-iodo-α-methyl-L-tyrosine SPECT in brain tumors. J Nucl Med 2004;45:374–381.